JOURNAL OF VIROLOGY, Nov. 2000, p. 10074–10080 Vol. 74, No. 21
0022-538X/00/$04.00+0

Human Immunodeficiency Virus Type 1 Spinoculation Enhances Infection through Virus Binding

UNA O'DOHERTY,[1,2] WILLIAM J. SWIGGARD,[1,3] AND MICHAEL H. MALIM[1,3]*

Departments of Microbiology,[1] Pathology and Laboratory Medicine,[2] and Medicine,[3] University of Pennsylvania School of Medicine, Philadelphia, Pennsylvania 19104-6148

Received 23 June 2000/Accepted 6 August 2000

The study of early events in the human immunodeficiency virus type 1 (HIV-1) life cycle can be limited by the relatively low numbers of cells that can be infected synchronously in vitro. Although the efficiency of HIV-1 infection can be substantially improved by centrifugal inoculation (spinoculation or shell vial methods), the underlying mechanism of enhancement has not been defined. To understand spinoculation in greater detail, we have used real-time PCR to quantitate viral particles in suspension, virions that associate with cells, and the ability of those virions to give rise to reverse transcripts. We report that centrifugation of HIV-1_{IIIB} virions at 1,200 × *g* for 2 h at 25°C increases the number of particles that bind to CEM-SS T-cell targets by ~40-fold relative to inoculation by simple virus-cell mixing. Following subsequent incubation at 37°C for 5 h to allow membrane fusion and uncoating to occur, the number of reverse transcripts per target cell was similarly enhanced. Indeed, by culturing spinoculated samples for 24 h, ~100% of the target cells were reproducibly shown to be productively infected, as judged by the expression of p24*^{gag}*. Because the modest *g* forces employed in this procedure were found to be capable of sedimenting viral particles and because CD4-specific antibodies were effective at blocking virus binding, we propose that spinoculation works by depositing virions on the surfaces of target cells and that diffusion is the major rate-limiting step for viral adsorption under routine in vitro pulsing conditions. Thus, techniques that accelerate the binding of viruses to target cells not only promise to facilitate the experimental investigation of postentry steps of HIV-1 infection but should also help to enhance the efficacy of virus-based genetic therapies.

The infectious life cycle of human immunodeficiency virus type-1 (HIV-1) is initiated when virions bind to susceptible target cells via the viral surface glycoprotein gp120/41^{env}. The fusion of the viral membrane with the target cell membrane is mediated through the interaction of Env with CD4 and members of the chemokine receptor family of proteins, most commonly CCR5 or CXCR4 (4). While Env interactions with these receptors are essential for virus infection, it is now appreciated that virus-cell binding may also be initiated through interactions with other cell surface molecules, such as heparan sulfate-containing proteoglycans (29, 32, 46) and the dendritic cell-specific intercellular adhesion molecule 3 binding C-type lectin DC-SIGN (17). Following membrane fusion, the viral core enters the cytosol, and a mysterious series of events that are collectively termed uncoating then ensues. These steps, which appear to include the shedding of p24^{gag} from the core, are presumably essential for formation of the viral nucleoprotein complex that mediates reverse transcription, transport to the nucleus, and integration of viral cDNA into the host genome to establish the provirus (13). Although these complexes have been described by various terms, we will refer to them broadly as postentry nucleoprotein, or reverse transcription (RT), complexes. Once the provirus is established, it serves as the template for subsequent virus gene expression, genome synthesis, and progeny virion production. Importantly, the relative efficiencies of these defined steps in HIV-1 replication have not been determined to a high degree of accuracy. As a consequence, the underlying reasons for the low infectivity-to-particle ratios that are usually assigned to HIV-1 (for example, 1 in 3,500 to 60,000 [26, 36]) are not well understood.

In an effort to address these points, we have been exploiting kinetic (real-time) PCR and RT-PCR to quantitate viral nucleic acids during the progressive stages of single-cycle HIV-1 infection. Early on in these studies, we found that our infection efficiencies were substantially enhanced by spinoculation, or centrifugal infection, techniques. Although such protocols have been used in clinical microbiology since the 1950s (18) to enhance infection by a number of difficult-to-culture pathogens (24), including HIV-1 (20, 37) and other retroviruses (3, 5), the mechanism whereby centrifugation leads to an enhanced level of infection remains controversial (24). Specifically, some groups have proposed that centrifugation enhances cellular susceptibility (22, 23) or viral fusion (43), whereas others have suggested that increased viral deposition is the most important aspect of centrifugal enhancement of infection (21, 34). With these uncertainties in mind, we decided to extend our quantitative analyses of virus binding, entry, reverse transcription, and particle production to investigate how spinoculation works. In summary, we demonstrate that centrifugal inoculation increases infection of T cells by HIV-1 mostly by depositing large numbers of virions on target cell surfaces in a CD4-dependent manner.

MATERIALS AND METHODS

Cell lines and viruses. The CD4-positive T-cell lines CEM-SS, HUT 78, and SupT1 were maintained as described previously (16, 33, 40, 41). Wild-type HIV-1_{IIIB} virus stocks were initially generated by transfection of 293T cells with the pIIIB infectious molecular clone (15), whereas the G glycoprotein of vesicular stomatitis virus (VSV G)-pseudotyped stocks were produced by cotransfection with pIIIB/Δ*env* (39) and pHIT/G (14). At 24 h, virus-containing supernatants were centrifuged at 500 × *g* for 10 min, treated with 30 μg of DNase I (Roche Biochemical)/ml for 30 min at room temperature in the presence of 10 mM $MgCl_2$, filtered through 0.45-μm-pore-size filters, and stored in aliquots at −80°C. CEM-SS cells were then infected with wild-type virus, and high-titer

* Corresponding author. Mailing address: Department of Microbiology, University of Pennsylvania School of Medicine, 347B Clinical Research Bldg., 415 Curie Blvd., Philadelphia, PA 19104-6148. Phone: (215) 573-3493. Fax: (215) 573-2172. E-mail: malim@mail.med.upenn.edu.

DNaseI-treated stocks were prepared as described above at the time of peak virus production. Importantly, we used HIV-1_{IIIB} stocks that had been passed through CEM-SS cells in an effort to minimize the presence of contaminating plasmid DNA. In several experiments, freshly thawed viral stocks were additionally passed through 0.2-μm-pore-size filters immediately prior to use to ensure the removal of any viral aggregates that might have formed.

Inoculation with HIV-1 at ambient gravity and at 1200 × *g*. As shown in the flow diagram of the centrifugal inoculation process (see Fig. 1), 2×10^5 cells per well in flat-bottom 96-well microtiter plates were incubated with 100 μl of viral stock (0.45 to 3.0 μg of $p24^{gag}$/ml). Plates were enclosed in plastic bags and centrifuged in microtiter plate carriers at 1,200 × *g* for 2 h at 25°C, and the cells were washed five times with cold medium. Control cells were incubated on a laboratory bench for the same time period and then washed similarly. Cell-associated viral RNA, DNA, and $p24^{gag}$ were assayed immediately (see below). After 5 or 24 h of culture, total viral DNA and $p24^{gag}$ were also measured. In some experiments, mixing (25 rotations/s) of virus-cell suspensions at ambient gravity for 2 h was performed using level 2 on a Vortex Genie 2 mixer (Scientific Industries Inc.). For other experiments, virus challenges were performed in the presence of the anti-CD4 mouse immunoglobulin G1 (IgG1) monoclonal antibody 19, which blocks HIV-1 infection (12), or 8 μg of polybrene/ml (Sigma Biochemicals).

Indirect immunofluorescence. Cytocentrifuged cells were prepared from infected cultures 24 h after inoculation and then fixed and permeabilized with 2% paraformaldehyde–1% Triton X-100. Samples were incubated with a polyclonal rabbit $p24^{gag}$-specific antiserum (38) followed by a fluorescein isothiocyanate-conjugated $F(ab')_2$ polyclonal goat anti-rabbit IgG antibody (Jackson Laboratories). The nuclei were counterstained with 4′,6′-diamidino-2-phenylindole (Vector Laboratories), and the samples were visualized at a magnification of ×400 using a Nikon Microphot-SA microscope with a cooled charge-coupled device camera (Princeton Instruments) and Metamorph image analysis software (Universal Imaging).

Measurement of cellular and viral RNA. Total cell-associated RNA (which includes viral RNA associated with cell surfaces as well as intracellular RNA) was prepared by lysis of 10^5 infected or uninfected cells in 1 ml of TRIZOL reagent (Life Technologies, Gibco BRL) with excess glycogen as a carrier (Roche Molecular Biochemicals), according to the manufacturer's instructions (6). RNA was similarly prepared from viral stocks by adding 10 μl of viral stock to 1 ml of TRIZOL.

Kinetic (fluorescence-monitored) RT-PCR (19) was performed using 1.25×10^4 cell equivalents to measure viral *gag* RNA and cellular glyceraldehyde-3-phosphate dehydrogenase (GAPDH) RNA, using molecular beacon technology (19) on an ABI-7700 kinetic PCR instrument (PE BioSystems). The sequences of the forward and reverse GAPDH and *gag* primers were 5′-TTCGCTCTCTGC TCCTCCTG-3′, 5′-ACCCGTTGACTCCGACCTTC-3′, 5′-ATAATCCACCTA TCCCAGTAGGAGAAAT-3′, and 5′-TTTGGTCCTTGTCTTATGTCCAGA ATGC-3′, respectively. The molecular beacon sequences for GAPDH and *gag* were 5′-GCGAGCAGCCACATCGCTCAGACACCATGGGCTCGC-3′ and 5′-GCGAGCCTGGGATTAAATAAAATAGTAAGAATGTATAGCGCTCG C-3′, labeled at the 5′ termini with the reporter fluorochrome 6-carboxyfluorescein and at the 3′ termini with the short-range quencher DABCYL (4-[4′-dimethylamino-phenylazo]-benzene) (Midland Certified Reagent Company). Reactions were carried out in 50-μl volumes containing 50 mM KCl, 10 mM Tris-HCl (pH 8.3), 5.5 mM $MgCl_2$, 300 μM (each) dATP, dCTP, dGTP, and dTTP, 200 or 900 nM forward primer, 200 or 900 nM reverse primer, 50 to 200 nM probe, 0.025 U of AmpliTaq Gold (PE BioSystems)/μl, 0.5 U of Moloney murine leukemia virus reverse transcriptase (Gibco BRL Life Technologies)/μl, and 500 nM carboxy-X-rhodamine as a passive reference (Molecular Probes). The reaction times and temperatures were 30 min at 48°C, 5 min at 95°C, and then 40 cycles of 15 s at 95°C and 45 s at 60°C.

A standard curve for viral RNA was prepared using serial dilutions of a synthetic *gag* transcript in 10 mM Tris-HCl (pH 8.0)–1-ng/ml polyriboadenylate carrier (Amersham Pharmacia Biotech)/ml. This RNA was synthesized using a DNA template that contained the *Hin*dIII-*Hin*dIII 627-bp restriction fragment of pIIIB *gag* (positions 1083 to 1710) and T7 polymerase (Promega). Unincorporated nucleotides were removed from the reaction using silica spin columns (RNeasy system; Qiagen), and the RNA concentration was determined by calculating the absorbance at 260 nm. To correct for variations in cell numbers and RNA recovery, a standard curve for cellular GAPDH RNA was generated by preparing RNA from uninfected CEM-SS cells that had been counted using a hemacytometer. These cell counts were then used to design serial dilutions of RNA in 10 mM Tris-HCl (pH 8.0)–1-ng/ml polyriboadenylate.

Sequence Detection software (version 3; PE BioSystems) was used to analyze the kinetic PCR amplification data.

Measurement of cell-associated viral DNA. Cell-associated DNA was prepared from 10^5 infected CEM-SS cells, by lysis in 100 μl of 10 mM Tris-HCl (pH 8.0)–1 mM EDTA–0.2 mM $CaCl_2$–0.001% Triton X-100–0.001% sodium dodecyl sulfate–1-mg/ml proteinase K. The lysates were then incubated at 58°C for 1 h, heat inactivated at 95°C for 15 min, and stored at −80°C. Kinetic (fluorescence-monitored) PCR was performed on 1.25×10^4 cell equivalents to quantitate viral *gag* DNA and cellular β-globin DNA. The sequences of the β-globin forward and reverse primers were 5′-CCCTTGGACCCAGAGGTTCT-3′ and 5′-CGAGCACTTTCTTGCCATGA-3′, and the molecular beacon, which was labeled with JOE (6-carboxy-4′,5′-dichloro-2′,7′-dimethoxyfluorescein) and DABCYL, was 5′-GCGAGCATCTGTCCACTCCTGATGCTGTTATGGGCG CTCGC-3′. The reaction and cycling conditions were the same as for RT-PCR, except that the concentration of $MgCl_2$ was 3 mM and reverse transcriptase and the initial 48°C incubation were omitted. A standard curve for the HIV-1 DNA copy number was prepared from mixtures of ACH-2 cells (which harbor two HIV-1 proviruses) and CEM-SS cells, using the above lysis procedure. In some experiments, a standard curve was also prepared by diluting pIIIB DNA in a CEM-SS cell lysate.

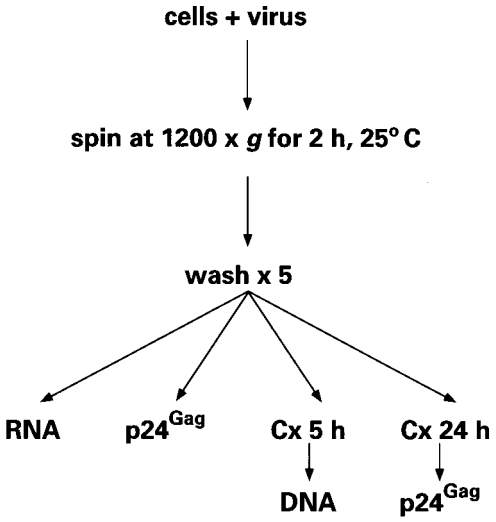

FIG. 1. Flow diagram of spinoculation; see the text for details. Cx, time in culture.

Measurement of cell-associated and supernatant $p24^{gag}$. Cell suspensions or corresponding supernatants were treated with 0.5% Triton X-100, and $p24^{gag}$ was quantitated using an enzyme-linked immunosorbent assay (ELISA) (NEN Life Science Products). Importantly, cell-associated $p24^{gag}$ represents the sum of the surface-bound and intracellular Gag antigen.

Calculation of virion equivalents from $p24^{gag}$ concentration. Virion equivalents were determined by assuming that there are an average of 1,500 molecules of $p24^{gag}$ present per viral particle (49) and that the molecular mass of $p24^{gag}$ is 25.587 kDa for HIV-1_{IIIB}. This equates to ~15,800 viral particles per pg of $p24^{gag}$, such that a viral stock of 3.0 μg of $p24^{gag}$/ml should represent 4.7×10^{10} virions per ml (or 9.4×10^{10} genomes per ml). In agreement with this, RT-PCR analysis (in triplicate) showed that the RNA copy number for a 3.0-μg/ml $p24^{gag}$ stock was $7 \times 10^{10} \pm 4 \times 10^{10}$ genomes per ml.

Calculation of virion sedimentation time. The time ($t = k/S$) required for the sedimentation of HIV-1 viral particles was calculated using established formulas for calculating k values [$k = \ln (r_{max}/r_{min})/\omega^2$], where ω is the angular velocity of the rotor in radian/s and r_{max} and r_{min} are the maximum and minimum radii (2) (J. Condino, Beckman publication, Beckman Instruments, Inc., Fullerton, Calif., 1996) and assuming that HIV-1 virions share with other retroviral particles a sedimentation coefficient of 600S (600×10^{-13} s) (48).

RESULTS

Spinoculation dramatically increases the adsorption of HIV-1 to T cells. To address the mechanistic basis for the enhancement of virus infection by centrifugal inoculation, we devised the experimental scheme outlined in Fig. 1. Here, the human T-cell line CEM-SS was incubated with a concentrated stock of HIV-1_{IIIB} at 25°C for 2 h at either 1 × *g* or 1,200 × *g* (spin conditions). Of note, these centrifugation conditions had no effect on cell viability as judged by trypan blue exclusion (data not shown). After extensive washing to remove unbound virions, the mean numbers of viral RNA copies, viral cDNA copies (extended minus-strand reverse transcripts), and virion equivalents of $p24^{gag}$ associated per cell were measured by RT-PCR, PCR, and ELISA, respectively (zero time point). The cells were then cultured at 37°C for 5 h, and the average number of copies of viral cDNA within each cell was determined. Normalization for the number of cell equivalents present in each sample was achieved through measuring GAPDH mRNA and β-globin DNA. Finally, after a total of

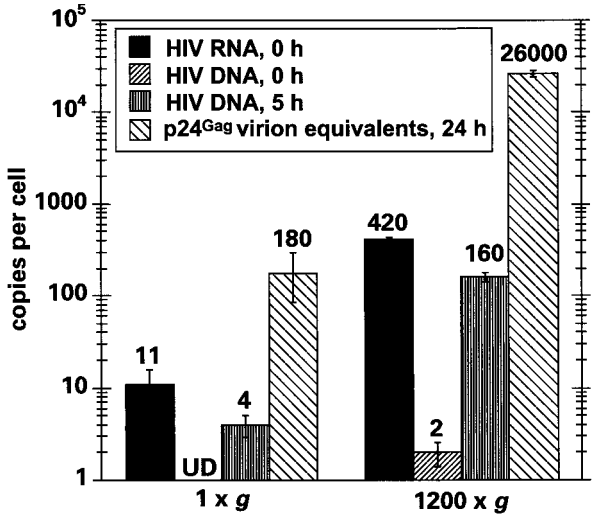

FIG. 2. Spinoculation enhances HIV-1 viral adsorption to CEM-SS cells and RT to similar extents. The numbers of copies of viral RNA and cDNA (extended first strand) per cell were measured immediately after challenge of 2×10^5 cells with 100 μl of a 3.0-μg/ml $p24^{gag}$ stock of HIV-1_{IIIB} at $1 \times g$ or $1,200 \times g$ using kinetic PCR. The numbers of copies of viral cDNA per cell were also measured after 5 h in culture. At 24 h, total levels of $p24^{gag}$ (cell associated and supernatant) were determined by ELISA and converted to the number of viral particles produced per cell. UD, undetectable.

24 h in culture, the mean $p24^{gag}$ protein production per cell was determined by ELISA and again converted to the number of virion equivalents. In most experiments, 95% confidence intervals were estimated after the assays were performed in triplicate.

Figure 2 illustrates the viral RNA and cDNA copy numbers per cell obtained at the zero time point, the cDNA copy numbers for the 5-h time point, and the estimated number of virions produced at 24 h, calculated from the amount of p24 in the culture supernatant. Corresponding values obtained for initially bound virions using $p24^{gag}$ as the measure were typically within twofold of those noted when quantitating viral RNA and are therefore not shown. Following spinoculation, it is very clear that the levels of cell-associated viral RNA were increased ~40-fold (420/11) over those seen for challenges performed at ambient gravity. Five hours later, the mean viral *gag* cDNA content per cell was similarly enhanced (160/4). Because only trace levels of viral DNA were detected immediately following the pulse, the bulk of these reverse transcripts must represent the synthesis of new, infection-initiated viral cDNAs.

From these observations we have concluded the following. (i) The conversion of cell-bound HIV-1 RNA to cDNA is very efficient under the two experimental conditions used here (>50% when one considers that the diploid genomes of retroviruses are capable of giving rise to single proviruses); this indicates that virus entry, uncoating, and early reverse transcription can all occur with relatively high efficiency. (ii) Spinoculation does not appear to enhance the efficiency of the stages of HIV-1 infection that closely follow virus binding; in particular, the conversion of cell-associated RNA to cDNA occurs with a similar efficiency irrespective of the *g* forces used during inoculation. (iii) The proportion of suspension viral particles that bind to target cells is quite low; specifically, even under the spinoculation conditions employed here, about 2% of the starting inoculum became cell associated. We appreciate that this figure may represent an underestimation of binding efficiency, since this calculation was made using the assumption that all viral RNA in the input inoculum was present in the form of binding-competent virus. We did find that the percentage of viral RNA that bound to cells could be increased by prolonged centrifugation (up to 10% for an 8-h spin); however, the levels of infectivity were not enhanced over those obtained after 2-h inoculations (data not shown). Moreover, because CEM-SS cells do not form confluent monolayers, some viral particles are likely to have become adsorbed to the plastic surfaces of the culture vessel instead of the target cells.

We also noticed that spinoculation enhanced the levels of virus production approximately fourfold more than cDNA synthesis when measured at 24 h (Fig. 2). This suggests that the high multiplicities of infection that are achieved through centrifugal inoculation may improve the efficiency of one or more intracellular steps of replication, perhaps by accelerating the accumulation of a viral gene product such that a required threshold level is attained more rapidly. An alternative interpretation could have been that centrifugation itself enhanced replication by inducing a hyperinfectable state; this possibility was ruled out by the demonstration that centrifugation of the target cells either before or after the application of virus did not enhance viral binding or production (data not shown).

Spinoculation can result in 100% productive infection of susceptible T cells in a single cycle. To determine the percentage of cells that became productively infected with HIV-1 following spinoculation, cytocentrifuge preparations of the infected cultures analyzed above were subjected to indirect immunofluorescence using a Gag-specific antiserum at 24 h postchallenge (Fig. 3). When the target cells were exposed to concentrated virus (4.7×10^9 virions per 2×10^5 cells in 100 μl) by spin infection, essentially 100% of the cells were expressing significant levels of viral antigen and the culture contained numerous syncytia (Fig. 3A). This contrasts with the infection at $1 \times g$, for which only 5 to 10% of the cells were visibly expressing Gag (Fig. 3B). The increased cell-associated p24 is unlikely to represent input virus, since total $p24^{gag}$ as measured by ELISA (cell-associated plus supernatant $p24^{gag}$) increased 24-fold over input levels in the spinoculated cultures during 24 h of culturing.

Modest *g* forces (1,200 × *g* for 2 h) are sufficient to sediment HIV-1 virions. As discussed earlier, a variety of mechanisms have been proposed to explain centrifugal enhancement of viral infection (21–24, 34, 35, 43). Because our results show that HIV-1 infection is significantly enhanced by spinoculation but that subsequent progression to cDNA accumulation is not further augmented (Fig. 2), it appeared most likely that this method works by simply depositing virions on target cell surfaces. On the other hand, and contrary to this notion, there has been some skepticism concerning the ability of viruses to be sedimented by the modest *g* forces used in spinoculation techniques (22). Because of these uncertainties, it was important for us to determine whether our centrifugation conditions resulted in virion sedimentation. Virus-containing supernatants of 100 μl were therefore incubated at 25°C at $1 \times g$ or $1,200 \times g$ for 2 h, and 20-μl fractions were then drawn serially from the top and assayed for $p24^{gag}$ content by ELISA (Fig. 4). Inspection of these data reveals that between 50 and 80% of the viral inoculum became concentrated in the lower 20% of the well volume following centrifugation. This concentrating effect occurred in the presence or absence of target cells, at 4 or 25°C, and with concentrated (900 ng of $p24^{gag}$/ml) and dilute (9 ng of $p24^{gag}$/ml) viral stocks (data not shown). Moreover, effective sedimentation was also maintained when virus stocks were passed through 0.2-μm-pore-size filters immediately prior to centrifugation, thus implying that virus aggregation was unlikely to be contributing to sedimentation (data not shown).

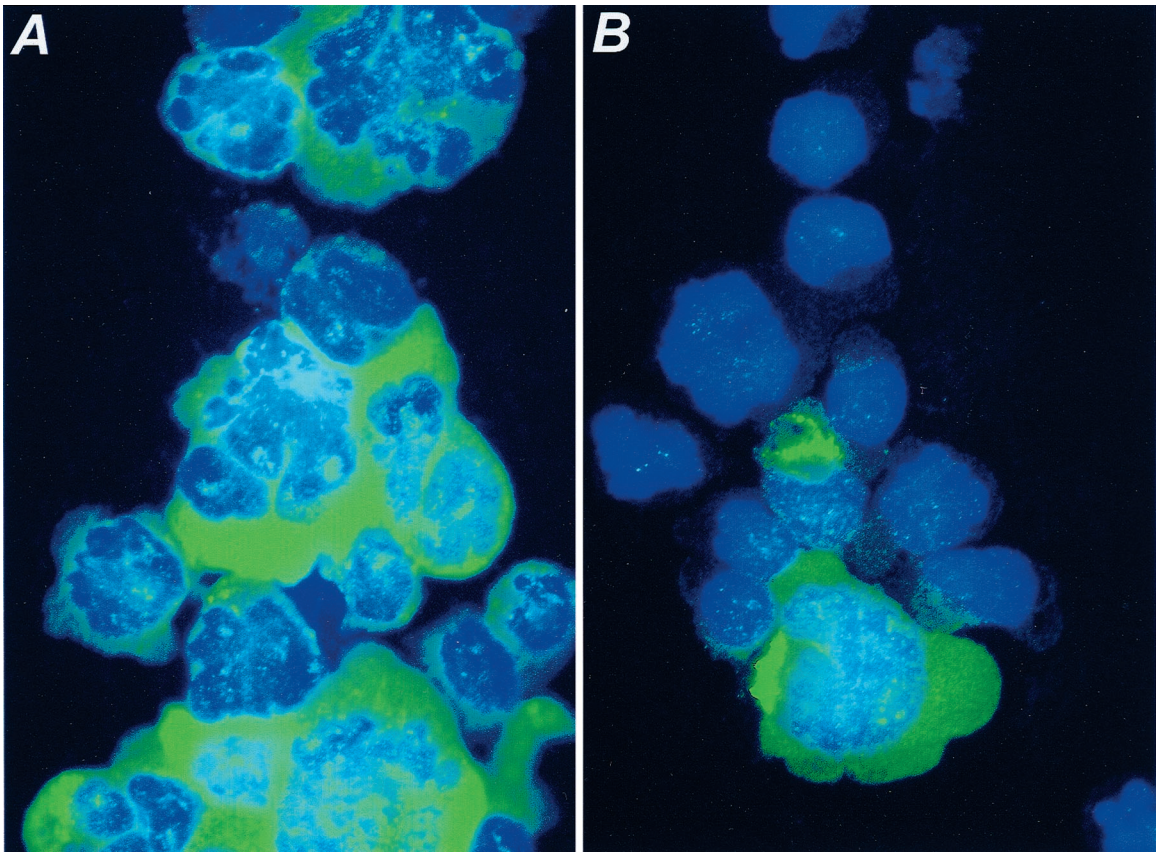

FIG. 3. Immunofluorescence analysis of CEM-SS cells infected at 1,200 × *g* (A) or 1 × *g* (B). Twenty-four hours after challenge, cells were fixed and stained with a $p24^{gag}$-specific antiserum followed by a fluorescein isothiocyanate-labeled secondary antibody. Cells were also stained with 4′,6′-diamidino-2-phenylindole and visualized at a magnification of ×400.

To validate the empirical observation that centrifugation at 1,200 × *g* for 2 h can sediment HIV-1 particles, we also calculated the predicted virion sedimentation time using a sedimentation coefficient of 600S (48). A viral suspension of 100 μl has a maximum depth of 5 mm in a 96-well microtiter plate; thus, using the Beckman GH3.7 rotor with a maximum radius of 168 mm and a minimum radius of 163 mm, the time for sedimentation at 2,500 rpm (41 rps) is calculated to be 7,355 s or approximately 2 h. This also explains why shorter centrifugation times resulted in proportionally less virus binding; for example, a 1-h spin resulted in a ~50% decrease in virus binding (data not shown).

Spinoculation selectively enhances CD4-dependent binding. Although HIV-1 entry generally requires the surface expression of CD4 and one of the chemokine coreceptors (42), a number of additional cell surface proteins can also serve as binding sites for HIV-1. In an effort to measure the specific contribution of CD4 to the binding of HIV-1 to CEM-SS cells under spinoculation conditions, we inoculated cells in the presence or absence of saturating doses of blocking anti-CD4 monoclonal antibodies (Fig. 5). Cell-associated $p24^{gag}$ was reduced by ~90% when the challenge was performed at 1,200 × *g*, indicating that spinoculation enhances CD4-selective binding to T cells to a greater extent than it enhances CD4-independent interactions. In contrast, CD4 blocking only reduced virus binding by approximately half at ambient gravity; this is broadly consistent with earlier work showing that a significant proportion of HIV-1 adsorption to cell surfaces can be CD4

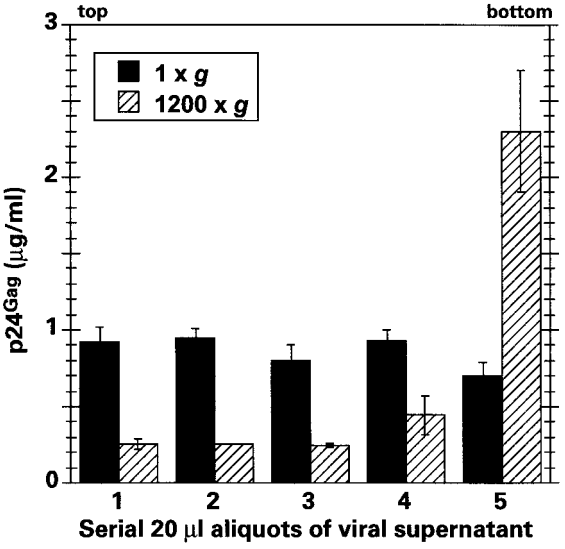

FIG. 4. The modest *g* forces used for spinoculation sediment HIV-1 particles. One-hundred-microliter aliquots of an HIV-1 viral stock were exposed to 1 × *g* or 1,200 × *g* for 2 h in a 96-well tissue culture microtiter plate at room temperature in the absence of cells. Serial 20-μl aliquots were then withdrawn from the upper meniscus and assayed for the presence of $p24^{gag}$ by ELISA. The data shown represent the means of three independent sample sets.

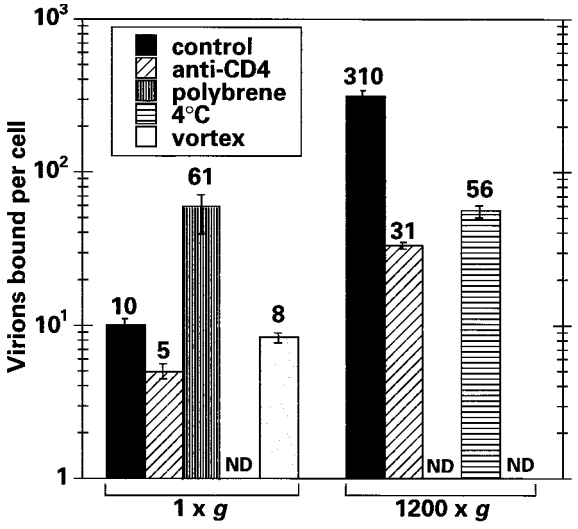

FIG. 5. Spinoculation-mediated virus binding is CD4 and temperature dependent. CEM-SS cells were challenged at 1 × *g* or 1,200 × *g* for 2 h under different conditions, and the levels of cell-associated p24^{gag} were determined immediately by ELISA and converted to numbers of virion equivalents. Control cells were inoculated in the presence of 10 μg of murine IgG1/ml at 25°C; the murine anti-CD4 IgG1 monoclonal antibody was present at a concentration of 10 μg/ml; polybrene was added to a final concentration of 8 μg/ml; temperature was maintained at 4°C; or cells were vortexed continuously during virus challenge (in this case, cell viability was shown to be maintained for the following 24 h). ND indicates that a particular combination of conditions was not tested.

independent under standard experimental conditions (27, 29, 32).

Polybrene enhances viral binding less than centrifugal inoculation. Polycations, such as polybrene, have been used for many years to enhance infection by HIV-1 and other viruses. Although this effect is thought to be mediated through increased viral adsorption as a consequence of decreasing repulsive forces (35) between virions and cells, a direct effect on HIV-1 binding has not been demonstrated (8, 44). When 8 μg of polybrene/ml was added to the 1 × *g* inoculation, the amount of cell-associated p24^{gag} was increased approximately sixfold over that for the control (Fig. 5). Thus, while virus adsorption was increased by polybrene, the effect was relatively minor in comparison to the 30- to 40-fold enhancements seen following spinoculation.

Spinoculation-enhanced binding is temperature dependent. To characterize the spinoculation-mediated procedure further, we also determined the effect of a reduction in temperature on cell-associated p24^{gag} levels. When all the centrifugation and washing steps were executed at 4°C, the levels were reduced approximately sixfold (Fig. 5). Because reducing the temperature to 4°C does not affect the sedimentation characteristics of HIV-1 (see above), we have concluded that the binding of virus to T cells most likely occurs more efficiently at the higher temperature (25°C)—a finding that agrees with the results of Ugolini and colleagues (45). Given that the majority of centrifugation-enhanced infection is CD4 dependent, this result might have been predicted, since earlier reports have demonstrated that the kinetics of HIV-1 Env binding to CD4 are slower at 4°C than at 37°C (9, 10, 28, 30, 31).

Vigorous mixing at ambient gravity does not enhance viral binding. The preceding experiments suggested to us that viral particle diffusion might be the limiting step for viral binding under standard infection conditions. To address this, virus-cell suspensions were gently vortexed at 25 rotations per s for 2 h at 25°C to assess whether continuous agitation could increase binding. Figure 5 clearly shows that this was not the case compared to results for a conventional stationary inoculation. Although not intuitive, these data are still consistent with diffusion being the major rate-limiting step for viral binding (discussed below).

Centrifugal inoculation enhances virus binding to a variety of T cells and with two different viral envelope proteins. Having shown that spinoculation enhances HIV-1$_{IIIB}$ particle adsorption to CEM-SS cells, we wished to confirm the generality of this mechanism by testing two additional T-cell lines, CD4-positive peripheral blood lymphocytes and HIV-1 cores pseudotyped with VSV G. Figure 6A shows that similar levels of p24^{gag} were associated with all three T-cell lines following challenge at 1 × *g* and that these levels were increased by similar orders of magnitude following spinoculation. Although

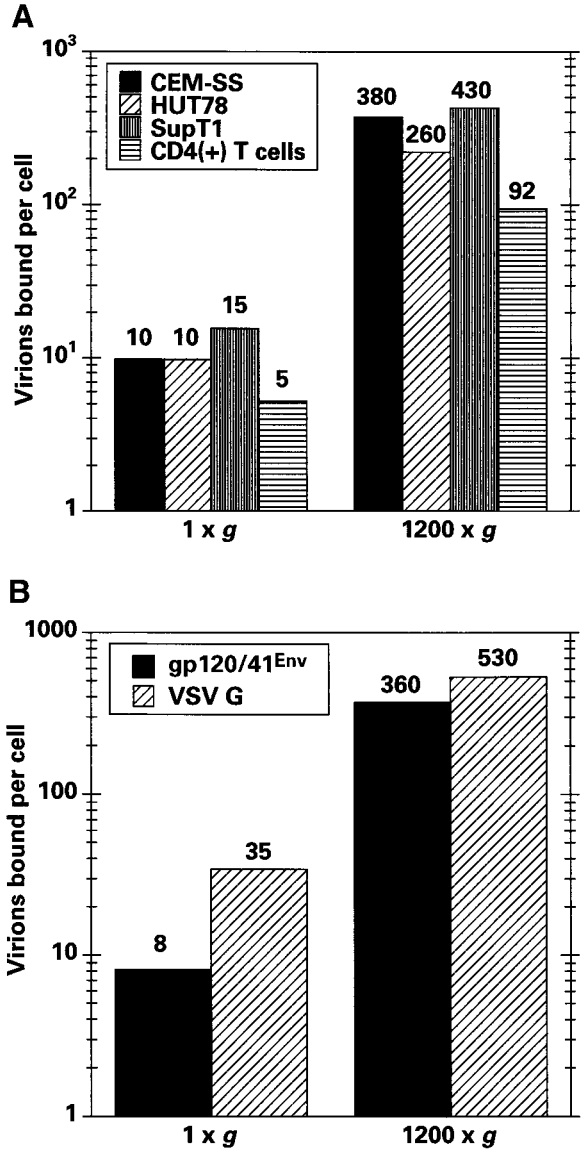

FIG. 6. Spinoculation enhances virus adsorption to different T cells and with VSV G pseudotypes. (A) The numbers of cell-associated virion equivalents following challenges of CEM-SS, HUT78, SupT1, or primary CD4-positive T cells were calculated as for Fig. 5. (B) Similarly, the effects of spinoculation were compared for HIV-1$_{IIIB}$ and HIV-1/Δ*env* (VSV G) pseudotypes.

primary T cells bound lower quantities of virus (perhaps as a consequence of having a smaller surface area), binding was still substantially increased by spin infection. Finally, we also challenged CEM-SS cells with virions pseudotyped with VSV G (Fig. 6B). Once again, cell-associated $p24^{gag}$ levels were substantially increased by spinoculation (~16-fold in this experiment), thus demonstrating that this technique can be extended to viral Env glycoproteins other than $gp120/41^{env}$.

DISCUSSION

Here we have utilized contemporary PCR-based methodologies to show that spinoculation enhances the CD4-dependent binding of HIV-1 to susceptible T-cell targets mainly by depositing increased numbers of virions onto the cells (Fig. 2). In other words, viral binding is a major rate-limiting step under routine pulsing conditions. The concomitant stimulation of viral infectivity does not appear to be due to a direct effect of centrifugation on the cells, nor does it appear to be due to an increased fusion efficiency, since spinoculation enhances the accumulation of reverse transcripts and virus binding to similar degrees (Fig. 2). While the initial steps of fusion and reverse transcription appear to be relatively efficient steps in the HIV-1 life cycle, the progression from the presence of reverse transcripts to fulminant viral infection is inefficient. For instance, for cells challenged under standard conditions, we found ~4 extended minus-strand cDNAs per cell (Fig. 2), yet only 5 to 10% of such cells became virus producers (Fig. 3). This equates to a cumulative efficiency of ~1% for the intervening steps of the life cycle and is very consistent with previous calculations made using alternative methods (25). The reasons that underlie this "loss" remain to be determined and may include inefficiencies during the completion of reverse transcription, nuclear transport, integration, or even transcription. Addressing these issues will likely shed light on the nature of the virus-host relationship during the postentry stages of virus infection; for example, it is possible that inefficiencies could be caused by any number of virion defects or cell-mediated antiviral phenotypes.

In experiments using a CD4-specific antibody we were able to demonstrate that the binding of virus to CEM-SS cells under spinoculation conditions is largely (~90%) CD4 dependent, whereas at $1 \times g$ binding is only partially (~50%) CD4 dependent (Fig. 5). We therefore propose that there may be a relatively small number of CD4-independent binding sites on CEM-SS T cells and that these can be readily saturated by centrifugal inoculation. In addition, we also found that the cell-associated levels of $p24^{gag}$ were reduced approximately sixfold when spinoculation was performed at 4°C (Fig. 5), even though viral particles are still sedimented at this lower temperature. As noted earlier, this finding is consistent with previous demonstrations of reduced binding of soluble CD4 to virions at 4°C (30, 31). It is also in keeping with the observation that the binding of Moloney murine leukemia virus to susceptible cells is less efficient at 4°C (50).

There are a number of factors that could, alone or in combination, contribute to this temperature effect. (i) As previously proposed, the binding of virions to cells may occur more slowly at 4°C, such that equilibrium would not be reached during the inoculation times used here. (ii) The efficiency of virus binding may be lower at 4°C. This could be the case if binding were to be stabilized by endothermic conformational changes in Env, CD4, or CXCR4. (iii) Virus binding may also be more stable at higher temperatures because of increased membrane fluidity, which would facilitate the interaction of multiple Env trimers from a single virion with the surface of one target cell. (iv) If virus binding were reversible, this would have a more dramatic effect on cell-associated $p24^{gag}$ levels (i.e., surface-bound and internalized $p24^{Gag}$) at 4°C where viral entry does not occur: challenges at higher temperatures result in membrane fusion and the uptake of Gag into the target cell cytoplasm.

We confirmed that bulk fluid agitation of virus and cells does not overcome the diffusion-imposed limitations to infection that are operative at ambient gravity (Fig. 5), as previously reported (1, 35, 47). This finding was to be expected, since the laminar boundary layers that are present close to the surfaces of cells in suspension are, like the mean viral displacement distance at $1 \times g$ (i.e., the distance that a virus is expected to move by diffusion within a half-life of 5 to 8 h), ~500 μm in depth (35). In other words, virus particles that are more than 500 μm from their target cells at the initiation of virus challenge do not contribute significantly to infection at $1 \times g$ (7). Thus, spinoculation apparently stimulates virus adsorption by imposing directionality on virus movement; in addition to improving the recovery of infectious virus from low-titer sources, centrifugal infections will be useful for infecting large numbers of cells synchronously, so that kinetic methods can be applied to the analysis of the early stages of HIV-1 infection, and for increasing the efficiency of retrovirus-mediated gene transfer.

Lastly, we speculate that in vivo conditions may surmount the limitation on the efficiency of HIV-1 infection that is imparted by diffusion in culture. In particular, direct contact between uninfected cells and cells producing (or carrying) virus particles will accelerate spread by substantially reducing the time between virus budding and the next round of binding. In keeping with this, it is well known that cell-to-cell infection by HIV-1 is much more efficient than infection with "cell-free" stocks (11). One cell type that is emerging as a critical participant during initial transmissions of HIV-1 and the subsequent establishment of vigorous and productive infections is the dendritic cell. These cells may bind and capture virions at sites of mucosal transmission and then migrate to T-cell-rich lymphoid tissues, where cell-to-cell contact would facilitate efficient viral transfer to highly permissive activated T cells.

ACKNOWLEDGMENTS

We thank Stylianos Andreadis, Paul Bates, Bob Doms, Jim Hoxie, Jeff Dvorin, Nathan Gaddis, John Moore, Farida Shaheen, and Alexandra Trkola for helpful discussions and Jim Hoxie for anti-CD4 antibodies.

The ABI-7700 is maintained through a core grant of the University of Pennsylvania Center for AIDS Research (AI45008), and the work was supported by U.S. Public Service grants AI41933 (to M.H.M.) and HL03984 (to U.O.).

REFERENCES

1. **Andreadis, S., T. Lavery, H. E. Davis, J. M. Le Doux, M. L. Yarmush, and J. R. Morgan.** 2000. Toward a more accurate quantitation of the activity of recombinant retroviruses: alternatives to titer and multiplicity of infection. J. Virol. **74:**1258–1266.
2. **Atkins, P. W.** 1994. Macromolecules, p. 795. Physical chemistry, 5th ed. W. H. Freeman and Company, New York, N.Y.
3. **Bahnson, A. B., J. T. Dunigan, B. E. Baysal, T. Mohney, R. W. Atchison, M. T. Nimgaonkar, E. D. Ball, and J. A. Barranger.** 1995. Centrifugal enhancement of retroviral mediated gene transfer. J. Virol. Methods **54:** 131–143.
4. **Berger, E. A., P. M. Murphy, and J. M. Farber.** 1999. Chemokine receptors as HIV-1 coreceptors: roles in viral entry, tropism, and disease. Annu. Rev. Immunol. **17:**657–700.
5. **Bunnell, B. A., L. M. Muul, R. E. Donahue, R. M. Blaese, and R. A. Morgan.** 1995. High-efficiency retroviral-mediated gene transfer into human and nonhuman primate peripheral blood lymphocytes. Proc. Natl. Acad. Sci. USA **92:**7739–7743.
6. **Chomczynski, P.** 1993. A reagent for the single-step simultaneous isolation of RNA, DNA and proteins from cell and tissue samples. BioTechniques **15:** 532–537.

7. **Chuck, A. S., and B. O. Palsson.** 1996. Consistent and high rates of gene transfer can be obtained using flow-through transduction over a wide range of retroviral titers. Hum. Gene Ther. **7:**743–750.
8. **Coelen, R. J., D. G. Jose, and J. T. May.** 1983. The effect of hexadimethrine bromide (polybrene) on the infection of the primate retroviruses SSV1/SSAV1 and BaEV. Arch. Virol. **75:**307–311.
9. **Dimitrov, D. S., K. Hillman, J. Manischewitz, R. Blumenthal, and H. Golding.** 1992. Correlation between kinetics of soluble CD4 interactions with HIV-1-Env-expressing cells and inhibition of syncytia formation: implications for mechanisms of cell fusion and therapy for AIDS. AIDS **6:**249–256.
10. **Dimitrov, D. S., K. Hillman, J. Manischewitz, R. Blumenthal, and H. Golding.** 1992. Kinetics of soluble CD4 binding to cells expressing human immunodeficiency virus type 1 envelope glycoprotein. J. Virol. **66:**132–138.
11. **Dimitrov, D. S., R. L. Willey, H. Sato, L. J. Chang, R. Blumenthal, and M. A. Martin.** 1993. Quantitation of human immunodeficiency virus type 1 infection kinetics. J. Virol. **67:**2182–2190.
12. **Endres, M. J., P. R. Clapham, M. Marsh, M. Ahuja, J. D. Turner, A. McKnight, J. F. Thomas, B. Stoebenau-Haggarty, S. Choe, P. J. Vance, T. N. Wells, C. A. Power, S. S. Sutterwala, R. W. Doms, N. R. Landau, and J. A. Hoxie.** 1996. CD4-independent infection by HIV-2 is mediated by fusin/CXCR4. Cell **87:**745–756.
13. **Fouchier, R. A. M., and M. H. Malim.** 1999. Nuclear import of human immunodeficiency virus type-1 pre-integration complexes. Adv. Virus Res. **52:**275–299.
14. **Fouchier, R. A. M., B. E. Meyer, J. H. M. Simon, U. Fischer, and M. H. Malim.** 1997. HIV-1 infection of non-dividing cells: evidence that the amino-terminal basic region of the viral matrix protein is important for Gag processing but not for post-entry nuclear import. EMBO J. **16:**4531–4539.
15. **Garrett, E. D., L. S. Tiley, and B. R. Cullen.** 1991. Rev activates expression of the HIV-1 *vif* and *vpr* gene products. J. Virol. **65:**1653–1657.
16. **Gazdar, A. F., D. N. Carney, P. A. Bunn, E. K. Russell, E. S. Jaffe, G. P. Schechter, and J. G. Guccion.** 1980. Mitogen requirements for the in vitro propagation of cutaneous T-cell lymphomas. Blood **55:**409–417.
17. **Geijtenbeek, T. B. H., D. S. Kwon, R. Torensma, S. J. van Vliet, G. C. F. van Duijnhoven, J. Middel, I. L. M. H. A. Cornelissen, H. S. L. M. Nottet, V. N. KewalRamani, D. R. Littman, C. G. Figdor, and Y. van Kooyk.** 2000. DC-SIGN, a dendritic cell-specific protein that enhances trans-infection of T cells. Cell **100:**587–597.
18. **Gey, G. O., F. B. Bang, and M. K. Gey.** 1954. Responses of a variety of normal and malignant cells to continuous cultivation and some practical applications of these responses to problems in the biology of disease. Ann. N. Y. Acad. Sci. **58:**976–999.
19. **Gibson, U. E. M., C. A. Heid, and P. M. Williams.** 1996. A novel method for real time quantitative RT-PCR. Genome Res. **6:**995–1001.
20. **Ho, W.-Z., R. Cherukuri, S.-D. Ge, J. R. Cutilli, L. Song, S. Whitko, and S. D. Douglas.** 1993. Centrifugal enhancement of human immunodeficiency virus type 1 infection and human cytomegalovirus gene expression in human primary monocyte/macrophages in vitro. J. Leukoc. Biol. **53:**208–212.
21. **Hodgkin, P. D., A. A. Scalzo, N. Swaminathan, P. Price, and G. R. Shellam.** 1988. Murine cytomegalovirus binds reversibly to mouse embryo fibroblasts: implications for quantitation and explanation of centrifugal enhancement. J. Virol. Methods **22:**215–230.
22. **Hudson, J. B.** 1988. Further studies on the mechanism of centrifugal enhancement of cytomegalovirus infectivity. J. Virol. Methods **19:**97–108.
23. **Hudson, J. B., V. Misra, and T. R. Mosmann.** 1976. Cytomegalovirus infectivity: analysis of the phenomenon of centrifugal enhancement of infectivity. Virology **72:**235–243.
24. **Hughes, J. H.** 1993. Physical and chemical methods for enhancing rapid detection of viruses and other agents. Clin. Microbiol. Rev. **6:**150–175.
25. **Kim, S., R. Byrn, J. Groopman, and D. Baltimore.** 1989. Temporal aspects of DNA and RNA synthesis during human immunodeficiency virus infection: evidence for differential gene expression. J. Virol. **63:**3708–3713.
26. **Kimpton, J., and M. Emerman.** 1992. Detection of replication-competent and pseudotyped human immunodeficiency virus with a sensitive cell line on the basis of activation of an integrated β-galactosidase gene. J. Virol. **66:**2232–2239.
27. **Marechal, V., F. Clavel, J. M. Heard, and O. Schwartz.** 1998. Cytosolic Gag p24 as an index of productive entry of human immunodeficiency virus type 1. J. Virol. **72:**2208–2212.
28. **Moebius, U., L. K. Clayton, S. Abraham, S. C. Harrison, and E. L. Reinherz.** 1992. The human immunodeficiency virus gp120 binding site on CD4: delineation by quantitative equilibrium and kinetic binding studies of mutants in conjunction with a high-resolution CD4 atomic structure. J. Exp. Med. **176:**507–517.
29. **Mondor, I., S. Ugolini, and Q. J. Sattentau.** 1998. Human immunodeficiency virus type 1 attachment to HeLa CD4 cells is CD4 independent and gp120 dependent and requires cell surface heparans. J. Virol. **72:**3623–3634.
30. **Moore, J. P., and P. J. Klasse.** 1992. Thermodynamic and kinetic analysis of sCD4 binding to HIV-1 virions and of gp120 dissociation. AIDS Res. Hum. Retrovir. **8:**443–450.
31. **Moore, J. P., J. A. McKeating, W. A. Norton, and Q. J. Sattentau.** 1991. Direct measurement of soluble CD4 binding to human immunodeficiency virus type 1 virions: gp120 dissociation and its implications for virus-cell binding and fusion reactions and their neutralization by soluble CD4. J. Virol. **65:**1133–1140.
32. **Moulard, M., H. Lortat-Jacob, I. Mondor, G. Roca, R. Wyatt, J. Sodroski, L. Zhao, W. Olson, P. D. Kwong, and Q. J. Sattentau.** 2000. Selective interactions of polyanions with basic surfaces on human immunodeficiency virus type 1 gp120. J. Virol. **74:**1948–1960.
33. **Nara, P. L., and P. J. Fischinger.** 1988. Quantitative infectivity assay for HIV-1 and -2. Nature **332:**469–470.
34. **Osborn, J. E., and D. L. Walker.** 1968. Enhancement of infectivity of murine cytomegalovirus *in vitro* by centrifugal inoculation. J. Virol. **2:**853–858.
35. **Palsson, B., and S. Andreadis.** 1997. The physico-chemical factors that govern retrovirus-mediated gene transfer. Exp. Hematol. **25:**94–102.
36. **Piatak, M., Jr., M. S. Saag, L. C. Yang, S. J. Clark, J. C. Kappes, J.-C. Luk, B. H. Hahn, G. M. Shaw, and J. D. Lifson.** 1993. High levels of HIV-1 in plasma during all stages of infection determined by competitive PCR. Science **259:**1749–1754.
37. **Pietroboni, G. R., G. B. Harnett, and M. R. Bucens.** 1989. Centrifugal enhancement of human immunodeficiency virus (HIV) and human herpesvirus type 6 (HHV-6) infection in vitro. J. Virol. Methods **24:**85–90.
38. **Simon, J. H. M., R. A. M. Fouchier, T. E. Southerling, C. B. Guerra, C. K. Grant, and M. H. Malim.** 1997. The Vif and Gag proteins of human immunodeficiency virus type 1 colocalize in infected human T cells. J. Virol. **71:**5259–5267.
39. **Simon, J. H. M., N. C. Gaddis, R. A. M. Fouchier, and M. H. Malim.** 1998. Evidence for a newly discovered cellular anti-HIV-1 phenotype. Nat. Med. **4:**1397–1400.
40. **Simon, J. H. M., D. L. Miller, R. A. M. Fouchier, M. A. Soares, K. W. C. Peden, and M. H. Malim.** 1998. The regulation of primate immunodeficiency virus infectivity by Vif is cell species restricted: a role for Vif in determining virus host range and cross-species transmission. EMBO J. **17:**1259–1267.
41. **Smith, S. D., M. Shatsky, P. S. Cohen, R. Warnke, M. P. Link, and B. E. Glader.** 1984. Monoclonal antibody and enzymatic profiles of human malignant T-lymphoid cells and derived cell lines. Cancer Res. **44:**5657–5660.
42. **Sodroski, J. G.** 1999. HIV-1 entry inhibitors in the side pocket. Cell **99:**243–246.
43. **Tenser, R. B., and M. E. Dunstan.** 1980. Mechanisms of herpes simplex virus infectivity enhanced by ultracentrifugal inoculation. Infect. Immun. **30:**193–197.
44. **Toyoshima, K., and P. K. Vogt.** 1969. Enhancement and inhibition of avian sarcoma viruses by polycations and polyanions. Virology **38:**414–426.

44a. **Tyagi, S., and F. R. Kramer.** 1996. Molecular beacons: probes that fluoresce upon hybridization. Nat. Biotechnol. **14:**303–308.

45. **Ugolini, S., I. Mondor, P. W. H. I. Parren, D. R. Burton, S. A. Tilley, P. J. Klasse, and Q. J. Sattentau.** 1997. Inhibition of virus attachment to $CD4^+$ target cells is a major mechanism of T cell line-adapted HIV-1 neutralization. J. Exp. Med. **186:**1287–1298.
46. **Ugolini, S., I. Mondor, and Q. J. Sattentau.** 1999. HIV-1 attachment: another look. Trends Microbiol. **7:**144–149.
47. **Valentine, R. C., and A. C. Allison.** 1959. Virus particle adsorption: theory of adsorption and experiments on the attachment of particles to non-biological surfaces. Biochim. Biophys. Acta **34:**10–23.
48. **Vogt, V. M.** 1997. Retroviral virions and genomes, p. 27–70. *In* J. M. Coffin, S. H. Hughes, and H. E. Varmus (ed.), Retroviruses. Cold Spring Harbor Laboratory Press, Cold Spring Harbor, N.Y.
49. **Vogt, V. M., and M. N. Simon.** 1999. Mass determination of Rous sarcoma virus virions by scanning transmission electron microscopy. J. Virol. **73:**7050–7055.
50. **Yu, H., N. Soong, and W. F. Anderson.** 1995. Binding kinetics of ecotropic (Moloney) murine leukemia retrovirus with NIH 3T3 cells. J. Virol. **69:**6557–6562.